Journal Pre-proof

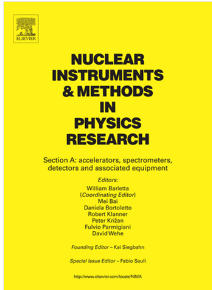

The capability of water Cherenkov detectors arrays of the LAGO project to detect Gamma-Ray Burst and high energy astrophysics sources

I. Sidelnik, L. Otiniano, C. Sarmiento-Cano, J.R. Sacahui, H. Asorey, A.J. Rubio-Montero, R. Mayo-Garcia, for the LAGO Collaboration

PII: S0168-9002(23)00565-X
DOI: https://doi.org/10.1016/j.nima.2023.168576
Reference: NIMA 168576

To appear in: *Nuclear Inst. and Methods in Physics Research, A*

Received date : 14 January 2023
Revised date : 30 June 2023
Accepted date : 11 July 2023

Please cite this article as: I. Sidelnik, L. Otiniano, C. Sarmiento-Cano et al., The capability of water Cherenkov detectors arrays of the LAGO project to detect Gamma-Ray Burst and high energy astrophysics sources, *Nuclear Inst. and Methods in Physics Research, A* (2023), doi: https://doi.org/10.1016/j.nima.2023.168576.

The capability of water Cherenkov detectors arrays of the LAGO project to detect Gamma-Ray Burst and High Energy Astrophysics sources

I. Sidelnik[a], L. Otiniano[b], C. Sarmiento-Cano[c], J. R. Sacahui[d], H. Asorey[a], A. J. Rubio-Montero[e], R. Mayo-Garcia[e], for the LAGO Collaboration[f]

[a] *Comisión Nacional de Energía Atómica (CNEA), Centro Atómico Bariloche, 8400 San Carlos de Bariloche, Argentina*
[b] *Comisión Nacional de Investigación y Desarrollo Aeroespacial (CONIDA)*
[c] *Universidad Industrial de Santander (UIS), Campus Bucaramanga, 28041 Bucaramanga, Colombia*
[d] *Universidad de San Carlos de Guatemala, Campus USAC, 01012 Ciudad de Guatemala, Guatemala*
[e] *Centro de Investigaciones Energéticas, Medioambientales y Tecnológica (CIEMAT), Centro de la Moncloa, 28040 Madrid, España*
[f] *https://lagoproject.org/collab.html*

Abstract

Gamma-Ray Bursts (GRBs) are one of the brightest transient events detected, with energies in their prompt phase ranging from keV to GeV. Theoretical models predict emissions at higher energies in the early times of the afterglow emission, and recently GRB190114C was the first GRB detected at TeV energies by the MAGIC experiment. The Latin American Giant Observatory (LAGO) operates a network of water Cherenkov detectors (WCD) at different sites in Latin America. Spanning over different altitudes and geomagnetic rigidity cutoffs, the geographic distribution of the LAGO sites, combined with the new electronics for control, atmospheric sensing, and data acquisition, allows the realization of diverse astrophysics studies at a regional scale. LAGO WCDs located at high altitudes possess good sensitivity to electromagnetic secondary radiation, which is the main expected signature of this kind of high-energy event on the ground. Due to the characteristics of the WCD and the wide field of view, LAGO possesses a large aperture high-duty cycle. In this work, we present the results of the sensitivity of LAGO small arrays of WCDs for the detection of events like GRB190114C. Also, we extend the study to other TeV galactic emitters, such as pulsar wind nebulas, TeV-halos, and some additional sources with unidentified categorizations. These are interesting sources to study taking advantage of the long-term monitoring capabilities of LAGO. We use a dedicated simulation process: ARTI, a toolkit developed by LAGO for high-energy air showers, MEIGA, a framework to simulate the response of the detectors, and oneDataSim, the new high-performance computing and cloud-based implementation of our simulation framework.

1. Introduction

Gamma-ray bursts (GRBs) are intense and transient events characterized by their high energies, typically ranging from keV to GeV. According to theoretical models, emissions from GRBs can extend up to TeV energies in the early afterglow phase. This prediction was confirmed by the detection of GRB 190114C by the MAGIC Collaboration, who reported the first definitive detection of a GRB in the energy range of 200 GeV to 1 TeV,[1]. The flux from this burst was observed at a significance level exceeding 50σ above the background within the first 20 minutes of the event. Another significant detection was made by the H.E.S.S. Collaboration from GRB 180720B, approximately ten hours after the initial prompt emission,[2]. They reported the detection of emissions from GRB 180720B in the energy range of 100–440 GeV. More recently, the LHASSO Collaboration detected GRB 221009A, providing the first detection of a photon with an energy of 18 TeV from a GRB,[3]. These observations confirm the existence of emissions from GRBs at energies reaching hundreds of GeV and beyond. It is worth noting that other sources, such as pulsar wind nebulae (PWN), TeV-halos, and certain unidentified galactic sources, are also known to emit photons with energies up to the TeV range. However, the observation of such sources is affected by the absorption of extragalactic background light (EBL) at these high energies. As a result, nearby sources have become particularly interesting for further study.

The Latin American Giant Observatory (LAGO) consists of a network of water Cherenkov Detectors (WCD) located at different sites in Latin America. One of the main objectives of LAGO is the detection of extreme events. Thanks to its wide field of view (FOV), LAGO constitutes a great facility for monitoring transient events like GRBs and long-term monitoring of steady sources such as PWN.

The LAGO WCD (Water Cherenkov Detector) consists of a sealed, light-tight container filled with water and equipped with optical detectors, typically an 8” to 9” photomultiplier tube (PMT). These detectors are in close contact to the water volume to register Cherenkov radiation. As Cherenkov photons are generated, they propagate through the water volume and can either be absorbed by the water or the inner coating of the container or reach the optical detector, resulting in the production of a variable number of photoelectrons (pe). These pe generate a current that is amplified in the corresponding stages of the optical detector, ultimately producing a pulse. In the LAGO detector network, an updated acquisition electronics system,[4] is currently

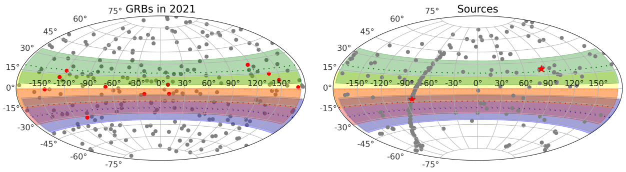

Figure 1: Left panel: GRBs observed during the year 2021 by the Fermi-GBM experiment. The colored bands represent the 15° field of view for five different high-altitude sites: Sierra Negra (SNG), San Antonio de Los Cobres (SAC), Chimborazo (CHI), Imata (IMA), and Atacama (ATA) (see Table 1). The red dots correspond to GRBs that were in the field of view of the high-altitude sites. Right panel: TeV known sources. The red stars correspond to the galactic center and GRB 190114C.

being deployed. This update allows for higher resolutions in both the temporal evolution of the measured pulses by the WCD and the obtained energy spectra. LAGO has also developed the ARTI toolkit,[5], a simulation framework that encompasses the simulation of the geomagnetic and atmospheric conditions, as well as the detectors' response to the flux of astroparticles. This toolkit includes the estimation of background radiation for each LAGO site. In light of recent detections made by MAGIC, the first stage of the LAGO simulation chain has been updated for the study of Gamma-Ray Bursts (GRBs).

2. Senstitivity to Gamma Ray Bursts

Several very high-energy astrophysical sources have been detected in the past decades both of galactic and extragalactic origins. These non-thermal photons are produced under extreme conditions. In the past few years, one of the most important discoveries was the detection of GRBs at these very high energies. GRBs are detected from all directions of the sky. The Gamma-Ray Burst Monitor (GBM) onboard the Fermi space telescope reports a rate of ∼240 events per year [6, 7]. Considering only the events from the years 2019–2020, we found that ∼12 events per year occurred within the 15° aperture FOV of each high-altitude detector of LAGO. In the left panel of Fig. 1, we display the GRBs that were observed by the GBM in the year 2021. Additionally, we include the GRBs that fell within the field of view (FOV) of five LAGO high-altitude sites located at an altitude greater than 4,500 meters above sea level (asl). These sites are listed in Table 1. The FOV band is projected in the 15° coloured bands centred in the local zenith. A wide FOV is reached when considering all the detectors measuring simultaneously, with good coverage of the galactic plane 1, right, making LAGO a great facility for detecting this kind of energetic GRBs.

We performed background and signal simulations at the five LAGO sites by using the ARTI [5] and oneDataSim [8] frameworks both designed by the LAGO Collaboration to take into account the different atmospheric and geomagnetic characteristics at each site and taking advantage of large high-performance computing and cloud-based facilities. In the first place, the background radiation expected at each site was calculated by using ARTI [5] with the standard atmospheric profile and the secular geomagnetic conditions for each location (see e.g., [9]).

Country	Site	Altitude [m asl]	Latitude [deg]	Longitude [deg]
Sierra Negra	SNG	4,550	18.2 N	97.9 W
Chimborazo	CHI	5,000	1.5 S	78.8 W
Imata	IMA	4,600	15.9 S	71.1 W
Atacama	ATA	5,100	23.0 S	67.8 W
S. A. de los Cobres	SAC	4,500	24.2 S	66.3 W

Table 1: Geographic location and altitude of five of the highest altitude LAGO sites. We evaluate the prospect of these five projected LAGO sites to study the high-energy component of GRBs and to detect the emissions of steady gamma sources in the TeV range.

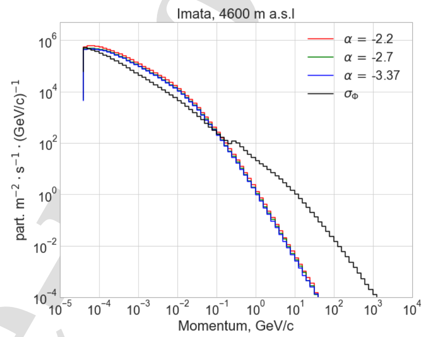

Figure 2: The secondary flux expected at 4,600 m asl in Imata, Peru, for the modelled GRB described in the text and for the three spectral indexes analyzed (coloured lines). Since the LAGO detector utilizes the single particle technique, the signals from GRBs can be observed above the background radiation fluctuations, depicted by the black curve. An energetic GRB would manifest as an increase in the flux within the electromagnetic dominated sector of the WCD's charge histogram.

The signals from Gamma ray sources were modelled by considering a power law, $E_p = j_0 E^{\alpha}$. To avoid statistical fluctuations, 10^5 photons were injected at the top of the local atmosphere at each site, within $0° \leq \theta \leq 15°$ and 0.2–1 TeV. Three different spectral indexes were considered: α=-2.20, α=-2.70 and α=-3.37. The resulting secondary flux was then normalised, using the GRB190114C as a reference, to properly account for the impact of the secondary radiation produced by the modelled GRB on the radiation background at each site. This is needed due to LAGO WCD are continuously monitoring the temporal evolution of the flux of secondary particles at the ground, and so, the observation of GRB signals are characterized by significant increases in the flux measured by the detector at characteristic times that are typically much shorter than the typical Poisson's variation of the background radiation. A comparison between the background Poissonian fluctuation and the secondary flux generated at each site by the modelled GRB was performed for the five sites studied (see table 1). An example of such comparison can be seen in Fig. 2 for the site of IMA at 4,600 m asl close to the town of Imata in Peru.

An array of three virtual detectors operating in coincidence was simulated at each site. Each detector response is obtained by using the Geant4-based simulation tool Meiga [10]. The resulting secondary particles that reach the ground are injected

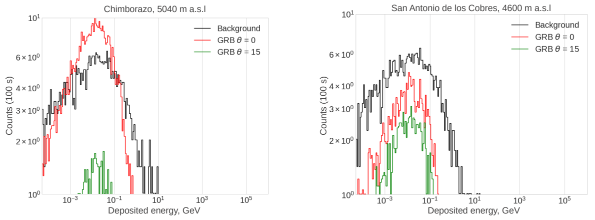

Figure 3: Simulated response of each WCD of a 3-detectors array operating in coincidence to the expected flux of signals of a 100 s burst as the one described in the text, $\theta = 0°$ (red line) and $\theta = 15°$ (green line) compared with the atmospheric radiation background (black line), for the sites of Chimborazo and San Antonio de Los Cobres.

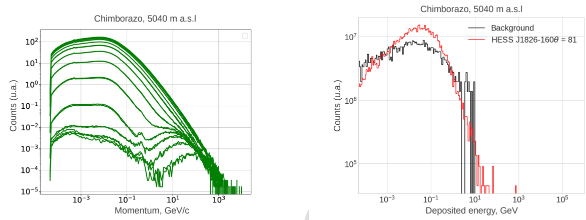

Figure 4: Secondary flux for different source elevations above the local horizon at Chimborazo (left), and the response of each WCD of an array of 3 detectors operating in coincidence (right) to the radiation background at the site (black) and the expected flux of the HESS J1826-130 gamma source at the moment of its maximum altitude above the local horizon.

into a virtual WCD with a diameter of $\phi = 1.58$,m and a height of $h = 1.50$,m. The water and coating optical properties were set and the resulting Cherenkov photons were propagated in the water and collected by an ellipsoidal volume emulating the 8” PMT. Photons are accounted for according to their wavelength and the corresponding quantum efficiency of the PMT. In Fig. 3, the expected coincidence signals for the GRB can be observed for two cases: $\theta = 0°$ and $\theta = 15°$, where θ represents the zenith angle. The coincident signals simultaneously detected in each one of the 3-WCD arrays during a 100 s burst can even exceed the total detected background at some sites.

3. Steady Gamma Sources

The design of the LAGO detection network covers a large range of latitudes from sites at close longitudes and allows the simultaneous and long-term observation of steady astrophysical sources from different places by using a superposed epoch analysis. With this method, background fluctuations can be largely reduced while the target signals continue to enhance as far as more data can be integrated. To study the feasibility of such a technique for the observation of point gamma sources, we study the signals flux expected from two steady gamma sources: the well-known Crab nebula and the recently observed HESS J1826-130 [11], identified with a star in the sources map of Fig. 1. To estimate the expected signal at each of the five sites studied, the local altitude (alt) of the source at each site was determined as a function of time in intervals of 30 minutes, and 10^5 photons following the energy distribution measured for each source were injected at the top of the atmosphere coming from the direction of the source, $\theta_S(t) = \pi/2 - \mathrm{alt}(t)$. For doing this, a special module in ARTI was developed and will be included in the next public release. As an example, in the left panel of Fig. 4, the obtained distribution at the ground for each position in the sky above the detector at 5,000 m asl in Chimborazo, Ecuador. It is clearly visible the atmospheric attenuation on the flux of secondary particles at the ground when different source altitudes are evaluated. For θ close to the horizon, the muonic component of the showers is less affected when compared with other components [5]. From this calculation, we determine a dynamic aperture $\Theta_S(E_{\mathrm{thr}})$, where E_{thr} is the minimum primary photon energy that can be detectable at each site, as the penetration depth of the incoming primary will depend on its energy once the site altitude is fixed and so the total number and the energy distribution of the secondaries at the detector level. The daily observation time of a particular source will be then defined by the criterion $t \mid \theta_S(t) \leq \Theta_S(E_{\mathrm{thr}})$, and so, by combining the energy detection threshold of the source at this site, the path of the source in the sky and the characteristics of the site, we are able to obtain the total integration time T needed for a source to be observable over the background. As an example, the Crab nebula can reach a maximum elevation of 66°26’, and so θ_{min} =23°34’ at our site of Chimborazo. For this zenith angle, our simulations show that the detection threshold should be $E_\gamma \simeq 1$ TeV, and this energy threshold remains up to θ_{min} =40°. It is possible to increase the FOV but only by incrementing the energy threshold, and so increasing the total integration time T. So, $\Theta_{\mathrm{Crab}}(1\,\mathrm{TeV}) = 40°$, and given the path of the Crab at Chimborazo, $t \simeq 5$ hours per day. Similar calculations show that the Crab at Sierra Negra can be detectable during $t \simeq 7$ hours per observation day. Given the flux, in all the studied sites, the integration times should be of several months of total integration times to reach a signal-to-background discrimination level for the Crab. Similar calculations can be done for the J1826-130 source, and as an example, the expected signals expected from this source compared with the background signals at the WCD can be seen in the right panel of Fig. 4 in Chimborazo, where it can be seen that a noticeable increment in the electromagnetic sector of the charge histogram of the WCD. Due to the lack of space, all the calculations for the LAGO capability detection for steady sources will be published in a follow-up work to the one presented here.

Acknowledgments

This work was partly carried out within the “European Open Science Cloud - Expanding Capacities by building Capabilities” (EOSC-SYNERGY) project, co-founded by the European Commission’s Horizon 2020 RI Programme under Grant Agreement nº 857647. We acknowledge the ICTP and OIEA grant NT-17 that partially founded stays to carry out this work. The LAGO Collaboration is very thankful to all the participating institutions and to the Pierre Auger Collaboration for their continuous support.

References

[1] MAGIC Collaboration, Teraelectronvolt emission from the γ-ray burst GRB 190114C, Nature 575 (7783) (2019) 455–458. doi:10.1038/s41586-019-1750-x.

[2] HESS Collaboration, A very-high-energy component deep in the γ-ray burst afterglow, Nature 575 (7783) (2019) 464–467. doi:10.1038/s41586-019-1743-9.

[3] Y. Huang, et al., LHAASO observed GRB 221009A with more than 5000 VHE photons up to around 18 TeV, GRB Coordinates Network 32677 (2022) 1.

[4] L. Arnaldi, et al., The new data acquisition system of the LAGO Collaboration based on the Redpitaya board, in: 2020 Argentine Conference on Electronics (CAE), IEEE, Buenos Aires, Argentina, 2020, pp. 87–92. doi:10.1109/CAE48787.2020.9046374.

[5] C. Sarmiento-Cano, et al., The ARTI framework: cosmic rays atmospheric background simulations, Eur. Phys. J. C 82 (2022) 1019. doi:10.1140/epjc/s10052-022-10883-z.

[6] C. Meegan, et al., The Fermi Gamma-ray Burst Monitor, Astroparticle Journal 702 (1) (2009) 791–804. doi:10.1088/0004-637X/702/1/791.

[7] A. von Kienlin, et al., The Fourth Fermi-GBM Gamma-Ray Burst Catalog: A Decade of Data, Astroparticle Journal 893 (1) (2020) 46. doi:10.3847/1538-4357/ab7a18.

[8] A. Rubio-Montero, et al., A Novel Cloud-Based Framework For Standardized Simulations In The Latin American Giant Observatory (LAGO), in: 2021 Winter Simulation Conference (WSC), IEEE, Phoenix, USA, 2021, pp. 1–12. doi:10.1109/WSC52266.2021.9715360.

[9] H. Asorey, S0_ima_86501_77402_QGSII_volu_defaults, Datasets from LAGO Observatory. EGI DataHub and LAGO Collab. (2021). URL http://hdl.handle.net/21.12145/lvSIHpk

[10] A. Taboada, et al., Meiga, a Dedicated Framework Used for Muography Applications, Journal for Advanced Instrumentation in Science 2022 (2022) 266. doi:10.31526/jais.2022.266.

[11] H. Abdalla, et al., An extreme particle accelerator in the Galactic plane: HESS J1826–130, Astronomy & Astrophysics 644 (2020) A112. doi:10.1051/0004-6361/202038851.